Ice2p is important for the distribution and structure of the cortical ER network in *Saccharomyces cerevisiae*

Paula Estrada de Martin[1,2], Yunrui Du[1,2], Peter Novick[2] and Susan Ferro-Novick[1,2,*]

[1]Howard Hughes Medical Institute, Yale University School of Medicine, New Haven, CT 06519, USA
[2]Department of Cell Biology, Yale University School of Medicine, New Haven, CT 06519, USA
*Author for correspondence (e-mail: susan.ferronovick@yale.edu)

Accepted 7 October 2004
Journal of Cell Science 118, 65-77 Published by The Company of Biologists 2005
doi:10.1242/jcs.01583

Summary

In *Saccharomyces cerevisiae*, the endoplasmic reticulum (ER) is found along the cell periphery (cortical ER) and nucleus (perinuclear ER). In this study, we characterize a novel ER protein called Ice2p that localizes to the cortical and perinuclear ER. Ice2p is predicted to be a type-III transmembrane protein. Cells carrying a genomic disruption of *ICE2* display defects in the distribution of cortical ER in mother and daughter cells. Furthermore, fluorescence imaging of *ice2Δ* cells reveals an abnormal cortical ER tubular network morphology in both the mother cell and the developing bud. Subcellular fractionation analysis using sucrose gradients corroborate the data from the fluorescence studies. Our findings indicate that Ice2p plays a role in forming and/or maintaining the cortical ER network in budding yeast.

Supplementary material available online at
http://jcs.biologists.org/cgi/content/full/118/1/65/DC1

Key words: Cortical ER, ER maintenance, Ice2p, *Saccharomyces cerevisiae*

Introduction

The endoplasmic reticulum (ER) is a polygonal network of membrane tubules and sheet-like cisternae (Palade, 1956). These tubular structures are connected to one another and to the outer nuclear envelope to form a continuous membranous system. In the budding yeast *Saccharomyces cerevisiae*, there are two types of ER: cortical (or peripheral) and perinuclear (Preuss et al., 1991; Rose et al., 1989). The cortical ER forms a network of interconnected tubules that is juxtaposed to the plasma membrane, whereas the perinuclear ER surrounds the nucleus (Prinz et al., 2000). Although it is complex in structure, the ER in higher eukaryotes is dynamic and undergoes continuous reorganization via the movement of individual tubules, ring closure of the tubular network and the formation of new tubules (Lee and Chen, 1988). In budding yeast, the cortical ER undergoes sliding and branching tubule movements, as well as those events reported for mammalian cells (Prinz et al., 2000).

The formation and maintenance of the tubular ER network in mammals requires microtubules (Terasaki, 1990; Terasaki et al., 1986), whereas, in plants, actin filaments play an important role in these events (Terasaki, 1990). Prinz et al. (Prinz et al., 2000) reported that the actin cytoskeleton is required for ER tubule network dynamics in yeast but not for ER network maintenance. The ER network in yeast and higher eukaryotic cells is highly dynamic. It extends to the cell periphery and is frequently rearranged when ER tubules fuse or when new ER tubules arise from pre-existing tubules (Prinz et al., 2000; Terasaki, 1990; Terasaki et al., 1986). The mechanisms regulating the formation and maintenance of the cortical ER tubular network remain to be elucidated. In this study, we identify a novel integral ER membrane protein called Ice2p, which plays a role in the formation and/or maintenance of the cortical ER tubular network in mother and daughter cells in budding yeast.

Materials and Methods

Plasmids and yeast strains

The construction of plasmids used to visualize the ER (Hmg1p-GFP, SFNB907; Sec61p-GFP, SFNB1492) and mitochondria [mitochondrial targeting sequence from the F_0 ATP synthase fused to red fluorescent protein (RFP), SFNB784] has been described previously (Cronin et al., 2000; Du et al., 2001; Hampton et al., 1996; Mozdy et al., 2000; Wiederkehr et al., 2003).

Strain SFNY1134 (Table 1) was constructed by transforming strain SFNY1128 with plasmid SFNB784 and selecting for Leu^+ transformants. Strain SFNY1494 (Table 1) was constructed by transforming strain SFNY1493 with plasmid SFNB798 after it was linearized with *Spe*I. Ura^+ transformants were then selected. To generate strains SFNY1491 and SFNY1492 (Table 1), plasmid SFNB1018 was digested with *Pml*I and introduced into strains NY873 and SFNY1493 (Table 1). Leu^+ transformants were then selected.

Strain SFNY1082 was constructed by tagging the C-terminus of YIL090w (ICE2) with the green fluorescent protein (GFP) according to the polymerase chain reaction (PCR)-based gene modification method of Longtine et al. (Longtine et al., 1998). The forward primer, FGFP090 (5′-CATTTTCTGTACTATTTTGGTATACGCTACAGA-ATTAATAGGTTCTGGTAGTCGGATCCCCGGGTTAATTAA-3′), contained 52 nucleotides of *ICE2* gene-specific sequence upstream of the stop codon and 20 nucleotides of gene-specific sequence from pFA6a-GFP(S65T)-His3MX6. The reverse primer, RGFP090 (5′-CGCGTATTTGGCAAAGCTGGTAATGCGGCTCTTTTGACAAT-GCATCAGCTGAATTCGAGCTCGTTTAAAC-3′), contained 50

Table 1. Yeast strains used in this study

Strain	Genotype	Source
NY873	*MATa his3-Δ200 lys2-801 leu2-3, 112 ura3-52*	Novick collection
SFNY1052	*MATa his3-Δ200 lys2-801 ura3-52::(URA3 HMG1-GFP) leu2-3, 112 ice2::(LEU2 ICE2::Tn3)*	This study
SFNY1054	*MATa his3-Δ200 lys2-801 leu2-3, 112 ura3-52::(URA3 HMG1-GFP)*	Ferro-Novick collection
SFNY1060	*MATα his3-Δ200 lys2-801 leu2-3, 112 ura3-52::(URA3 HMG1-GFP)*	Ferro-Novick collection
SFNY1061	*MATa/α his3-Δ200/his3-Δ200 lys2-801/lys2-801 leu2-3, 112/leu2-3, 112 ura3-52::(URA3 HMG1-GFP)/ ura3-52::(URA3 HMG1-GFP)*	Ferro-Novick collection
SFNY1082	*MATa lys2-801 leu2-3, 112 ura3-52 his3-Δ200 ICE2-GFP::his5+*	This study
SFNY1128	*MATa lys2-801 leu2-3, 112 ura3-52::(URA3 HMG1-GFP) his3-Δ200 ice2Δ::his5+*	This study
SFNY1134	*MATa lys2-801 leu2-3, 112 ura3-52::(URA3 HMG1-GFP) his3-Δ200 ice2Δ::his5+* pSFNB784 (*PPrFoATP-dsRFP, LEU2, CEN*)	This study
SFNY1135	*MATα lys2-801 leu2-3, 112 ura3-52::(URA3 HMG1-GFP) his3-Δ200 ice2Δ::his5+*	This study
SFNY1283	*MATa lys2-801 leu2-3, 112 ura3-52::(URA3 HMG1-GFP) his3-Δ200::(his5+ ICE2-13x-Myc)*	This study
SFNY1284	*MATa/α his3-Δ200/his3-Δ200 lys2-801/lys2-801 leu2-3, 112/leu2-3, 112 ura3-52::(URA3 HMG1-GFP)/ ura3-52::(URA3 HMG1-GFP) his3-Δ200 ice2Δ::his5+/his3-Δ200 ice2Δ::his5+*	This study
SFNY1449	*MATa/α his3-Δ200/his3-Δ200 leu2-3,112/ leu2-3,112 ura3-52::(URA3, HMG1ΔC-GFP)/ura3-52::(URA3, HMG1ΔC-GFP) SEC3::KanMx/ SEC3::KanMx*	Ferro-Novick collection
SFNY1491	*MATa his3-Δ200 lys2-801 ura3-52 leu2-3, 112::(LEU2 SEC61-GFP)*	This study
SFNY1492	*MATa lys2-801 ura3-52 leu2-3, 112::(LEU2 SEC61-GFP) his3-Δ200 ice2Δ::his5+*	This study
SFNY1493	*MATa lys2-801 leu2-3, 112 ura3-52 his3-Δ200 ice2Δ::his5+*	This study
SFNY1494	*MATa lys2-801 leu2-3, 112 ura3-52::(URA3 SEC7-GFP) his3-Δ200 ice2Δ::his5+*	This study
SFNY1497	*MATa his3-Δ200 lys2-801 leu2-3, 112 ura3-52::(URA3 HMG1-GFP)* pSFNB784 (*PPrFoATP-dsRFP, LEU2, CEN*)	This study
FY23	*MATa ura3-52 trp1-63 leu2-1*	W. Prinz*
WPY152	*MATa ura3-52 trp1-63 leu2-1 srp102-510*	W. Prinz*

*NIH, Bethesda, MD.

nucleotides of *ICE2* gene-specific sequence just downstream of the stop codon and 20 nucleotides of gene-specific sequence from the plasmid above. PCR was used to amplify the fragment and the PCR product was subsequently transformed into NY873 (Table 1). His$^+$ transformants were selected and fusion of the C-terminus of *ICE2* with GFP was determined by PCR.

The method developed by Longtine et al. (Longtine et al., 1998) was used to construct SFNY1284. To modify the C-terminus of *ICE2* with 13× Myc, ICE2F2MYC (5′-CTGTACTATTTTGGTATACGCT-ACAGAATTAATAGGTTCTGGTAGTCGGATCCCGGTTAATTAA-3′) was used as the forward primer and ICE2R1MYC (5′-TGGCAAAGCTGGTAATGCGGCTCTTTTGACAATGCATCAGC-TGAATTCGAGCTCGTTTAAAC-3′) as the reverse primer. ICE2F2MYC contained 46 nucleotides of *ICE2* gene-specific sequence upstream of the stop codon and ICE2R1MYC contained 42 nucleotides of *ICE2* gene-specific sequence downstream of the stop codon. Both primers contained 20 nucleotides of pFA6a-13myc-His3MX6 gene-specific sequence. The fragment was amplified by PCR, introduced into strain SFNY1054 and His$^+$ transformants selected. The gene modification was verified by PCR.

Isolation and cloning of TMT561

SFNY1054 was transformed with a library of yeast genomic DNA fragments containing insertions of a mini-Tn3*::LacZ::LEU2* transposon that were digested with *Not*I (Burns et al., 1994; Du et al., 2001). Leu$^+$ transformants were selected and examined for defects in cortical ER inheritance as described by Du et al. (Du et al., 2001).

Using a PCR-mediated method previously described in Du et al. (Du et al., 2001), the location of the transposon in TMT561 (SFNY1052) was determined and mapped to chromosome IX, between open reading frames (ORFs) YIL091c and YIL090w. To determine which ORF was affected by the transposon insertion, reverse-transcription PCR (RT-PCR) was performed using primers for YIL091c, YIL090w and *AUX1/SWA2* on RNA samples prepared from NY873 and TMT561. RNA was isolated from strains NY873 and TMT561 using the RNeasy Mini kit (Qiagen, Valencia, CA) and reverse transcription was performed using the Omniscript RT kit (Qiagen, Valencia, CA) in the presence of 40 U μl^{-1} RNase OUT Recombinant Ribonuclease Inhibitor (Invitrogen, San Diego, CA).

Disruption of ICE2

Strains SFNY1128 and SFNY1135 (Table 1) were constructed by a PCR-based gene disruption method (Longtine et al., 1998). The forward primer, TMT561F (5′-CTATTAGAGAGGTGCTGTTTGTG-GCCGATCACGCTAAAGATTAGGCAACGCGGATCCCCGGGTT-AATTAA-3′), and the reverse primer, TMT561R (5′-CGCGT-ATTTGGCAAAGCTGGTAATGCGGCTCTTTTGACAATGCATC-AGCTGAATTCGAGCTCGTTTAAAC-3′), each contain 50 nucleotides of *ICE2* gene-specific sequence upstream of the start codon and downstream of the stop codon, respectively. TMT561F and TMT561R each contain 20 nucleotides that correspond to gene-specific sequence from the plasmid pFA6a-His3MX6, which contains the *his5*$^+$ gene from *Schizosaccharomyces pombe* (Longtine et al., 1998). The *his5*$^+$ gene was amplified by PCR using TMT561F and TMT561R, and the product was transformed into strains SFNY1054 and SFNY1060. His$^+$ transformants were selected and the disruption of *ICE2* with *his5*$^+$ was confirmed by PCR.

Fluorescence microscopy

Cells were observed with a Zeiss Axiophot fluorescence microscope using a Zeiss 100× Plan-Apochromat oil-immersion objective. GFP and RFP/Cy3 fluorescence were detected with the 480-nm and 540-nm filters, respectively. Images were captured using an Orca ER digital camera (Model C4742-95, Hamamatsu Photonics, Hamamatsu City, Japan) and the OpenLab 3.08 imaging software (OpenLab, Lexington, MA). Images were processed with Photoshop 7.0 and Illustrator 10.0 (Adobe Systems, San Jose, CA).

To visualize the ER or mitochondria, cells expressing GFP or RFP fusion proteins were grown overnight in minimal medium with the appropriate amino acids at 30°C to an optical density at 600 nm (OD_{600}) of 0.6. Cells were then pelleted and resuspended in 50 μl of the appropriate medium. The cell solution (4 μl) was then mixed with an equal volume of growth medium containing the appropriate amino acids and 0.8% NuSieve GTG low-melting-

temperature agarose (FMC BioProducts, Rockland, ME) that was kept at 37°C.

Indirect immunofluorescence was performed according to Estrada et al. (Estrada et al., 2003).

Whole cell lysates

Cells (NY873 and SFNY1082) were grown overnight to an OD_{600} of 0.6 in yeast extract-peptone-dextrose (YPD) medium and samples were prepared and processed according to Ferreira et al. (Ferreira et al., 2002). Briefly, 2.5 ml of cells grown to an OD_{600} of 0.6 were harvested, resuspended in 500 µl water and lysed in 50 µl 1.85 M NaOH and 3.5% (v/v) β-mercaptoethanol. Proteins were precipitated by adding 50 µl cold 50% trichloroacetic acid and the resulting pellet was resuspended in 20 µl 1 M Tris and 30 µl sodium-dodecyl-sulfate (SDS) sample buffer. Samples were then analysed by SDS polyacrylamide-gel electrophoresis (SDS-PAGE).

Approximately 2.5 ml of cells grown to an OD_{600} of 0.6 were harvested, resuspended in 30 µl 1× SDS sample buffer and immediately boiled for 3 minutes at 100°C. Cells were lysed with glass beads by vortexing for 2 minutes in the presence of 1× SDS sample buffer. Lysates were then boiled for 1 minute at 100°C and samples subjected to SDS-PAGE.

Glycoprotein analysis

Yeast extracts were prepared from strains NY873 and SFNY1283 as described above, and treated with endoglycosidase H (EndoH; New England Biolabs, Beverly, MA) according to Friedmann et al. (Friedmann et al., 2002) and the supplier's instructions. Briefly, lysates were incubated with 1000 units EndoH for 16 hours at 25°C. Samples were then resolved on 10% SDS-PAGE gels and subjected to western blot analysis using anti-myc or anti-carboxypeptidase-Y (anti-CPY) antibodies (Friedmann et al., 2002).

Subcellular fractionation

Strains NY873, SFNY1128 and SFNY1283 were grown, lysed and fractionated using sucrose velocity gradients as described previously (Barrowman et al., 2000; Estrada et al., 2003). Lysates prepared from strains SFNY1280 and SFNY1494 were subjected to subcellular fractionation using sucrose density gradients according to Barrowman et al. (Barrowman et al., 2000). The protein in each fraction was precipitated with cold 50% trichloroacetic acid (TCA; chilled to 4°C) and prepared as described by Estrada et al. (Estrada et al., 2003). Samples were then resolved by SDS-PAGE and subjected to western blot analysis, and antigens were detected by enhanced chemiluminescence (ECL) (Amersham Pharmacia Biotech, Piscataway, NJ). Bands were quantified using BioImage software and the data were plotted as a proportion of the maximum antigenic material.

To resolve ER membranes from the plasma membrane, cells were grown and prepared as described previously (Estrada et al., 2003; Roberg et al., 1999; Roberg et al., 1997). The plasma membrane and ER from strains NY873 and SFNY1283 were fractionated on a linear sucrose density gradient in the presence of EDTA and ~440 µl fractions were collected from the top of the gradient. The protein in each fraction was subsequently precipitated with cold 50% TCA and processed as described by Estrada et al. (Estrada et al., 2003). The data were plotted as a proportion of the maximum antigenic material. Fig. S1 depicts scanned western blots from all sucrose gradients (see Fig. S1 in supplementary material).

Imaging of the ER network

ER network imaging of strains SFNY1061, SFNY1284 and SFNY1449 was performed on diploid cells grown at 30°C to an OD_{600} of 0.6 in minimal medium containing the appropriate amino acids. Live cells (1 ml) were harvested, resuspended in 50 µl of the appropriate medium, and 4 µl of the concentrated suspension were mounted in 4 µl 0.4% agarose. Cells were viewed with a Zeiss fluorescence microscope, a stack of images was obtained with focal planes ~2 µm apart and images were deconvolved using OpenLab 3.08 software. Images were processed further using Photoshop 7.0 and Illustrator 10.0.

Cycloheximide treatment

Wild-type and *ice2* mutant cells were grown at 30°C. The *srp102-510* mutant and its corresponding wild-type strain were grown at 25°C. All cells were grown to an OD_{600} of 0.5 in 50 ml of minimal medium with the appropriate amino acids. Cycloheximide (final concentration of 1 µM; Sigma-Aldrich, St Louis, MO) was added to half of each culture; wild-type and *ice2* mutant cells were incubated at 30°C for 6 hours, whereas *srp102-510* and its isogenic wild type were incubated for 6 hours at 37°C (Prinz et al., 2000). Cells were either subjected to fluorescence microscopy to examine the ER network or subcellular fractionation was performed.

Results

Isolation and cloning of TMT561

To identify components that are required for the maintenance or inheritance of the ER, cells expressing the ER marker Hmg1p-GFP (Du et al., 2001) were mutagenized by randomly inserting a Tn3-based transposon into the yeast genome as described previously (Burns et al., 1994). A total of 3331 transformants (numbered TMT1 to TMT3331) were visually screened for defects in the distribution of cortical ER in daughter cells and 17 mutants were identified. To determine whether the Tn3-based transposon inserted at a single locus, the mutants were crossed to a wild type strain (NY873). The resulting diploid cells were sporulated and ten tetrads were dissected. In the case of four of the mutants, the transposon insertion (marked by the *LEU2* gene) and the defect in cortical ER distribution co-segregated 2:2. The characterization of one of these mutants, now called *aux1/swa2*, has been reported previously (Du et al., 2001). In the case of two other mutants (TMT1246 and TMT1536), no phenotype was observed when the affected genes were disrupted. Here, we discuss the characterization of the fourth mutant, TMT561.

The ER distribution phenotype of TMT561 (SFNY1052, *ice2::Tn3*, Table 1) and wild-type cells was quantified in more than 170 small buds with a volume of 4-13% of the mother cell. Approximately 70% of the *ice2* cells displayed a defect in the delivery of ER into daughter cells (Fig. 1A, middle; Table 2), whereas less than 10% of wild-type cells failed to acquire cortical ER. Some of the mutant cells did not contain any ER in the bud (38%; Fig. 1A, middle, star), whereas others contained only a dot (21%; Fig. 1A, middle, arrow) or patch (13%; Fig. 1A, middle, arrowhead) of ER at the bud tip. When compared with the wild type, *ice2* cells (strain SFNY1052) also displayed less continuous peripheral staining of the ER in the mother cell. The phenotypes of the mutant suggested that Ice2p might play a role in the delivery of ER tubules to the periphery of the bud during isotropic growth, or it might play a role in maintaining the ER in both mother and daughter cells.

The location of the transposon insertion in TMT561 was mapped by a PCR-based method (Adams et al., 1997; Du et al., 2001) to chromosome IX between two hypothetical ORFs,

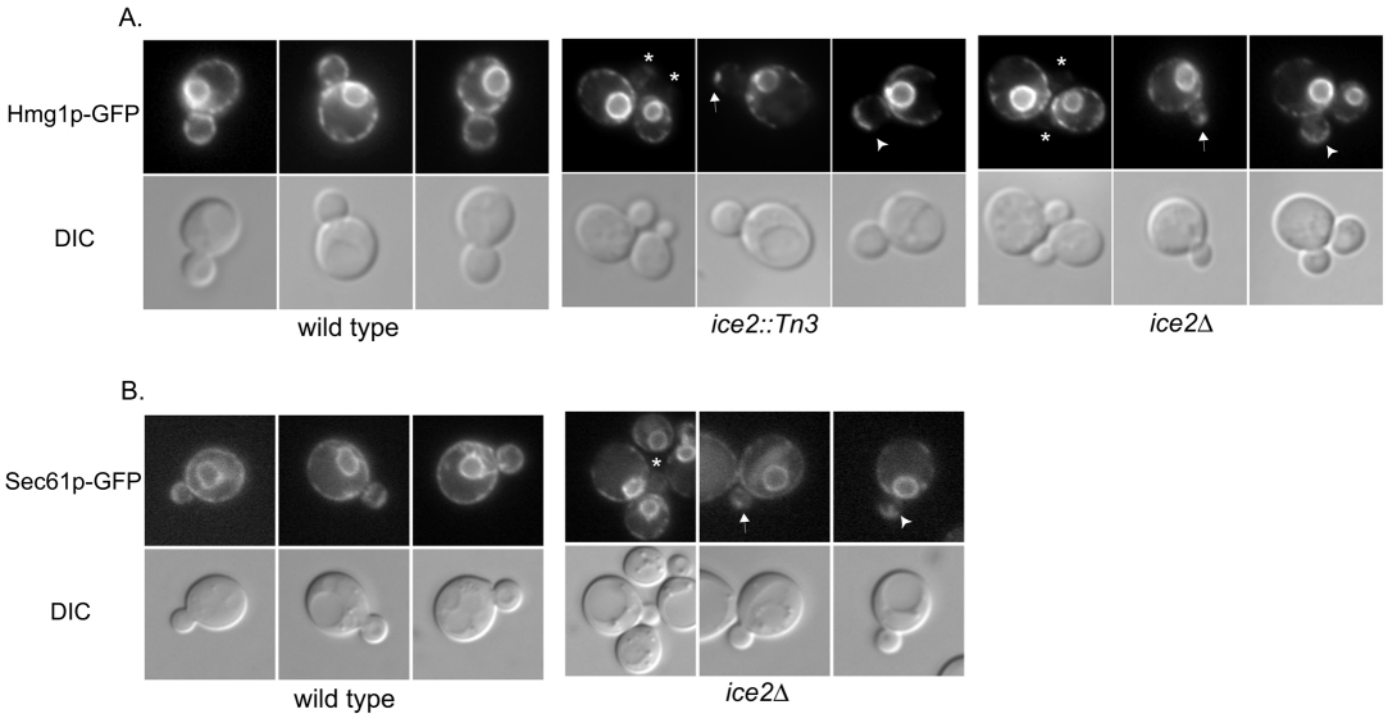

Fig. 1. The ER fails to distribute to the periphery of daughter cells in the absence of Ice2p. Wild-type and *ice2* mutant cells expressing the ER markers Hmg1p-GFP (A), or Sec61p-GFP (B) were grown at 30°C to early log phase in minimal medium with the appropriate amino acids. Asterisks indicate small buds in *ice2* cells without cortical ER; arrows and arrowheads point to buds with a concentration of ER at the tip. The ER distribution in small buds with a volume of 4-13% of the mother cell was analysed using fluorescence microscopy.

YIL091c and YIL090w (Fig. 2A). To resolve which gene product was affected by the transposon insertion, RT-PCR was performed using forward and reverse primers for YIL091c and YIL090w, respectively. cDNA templates from the wild type generated a 0.40 kb PCR product with primers for YIL090w (Fig. 2B, lane 2), and a 0.35 kb band with primers for YIL091c and the *AUX1/SWA2* ORF, which served as a positive control (Fig. 2B, lanes 3, 4, respectively). cDNA templates prepared from TMT561 produced a 0.35 kb PCR product with primers for YIL091c and the *AUX1/SWA2* ORF (Fig. 2B, lanes 6, 7, respectively), but the 0.40 kb band was absent when primers for YIL090w were used (Fig. 2B, lane 5).

To confirm that YIL090w is the affected ORF, RT-PCR was performed using increasing concentrations of the wild-type template (Fig. 2C, lanes 2-5) and 2000 ng of TMT561 RNA (Fig. 2C, lane 6). A light 400-bp band was detected in lane 2 using 20 ng of wild-type RNA as the template and the intensity of that band increased as more RNA was used in the reaction (Fig. 2C, lanes 3-5). The 0.40 kb PCR product was not detected using 2000 ng of TMT561 RNA template. This finding indicates that the transposon insertion specifically affected YIL090w and not the gene product of YIL091c.

Table 2. Quantitation of ER distribution in small buds* of wild-type and *ice2* mutants

	No ER in bud	'Dot' in bud	'Cap' in bud	ER in bud
Wild type (Hmg1p-GFP), *n*=221	9 (4%)	4 (2%)	5 (2%)	203 (92%)
ice2::Tn3 (Hmg1p-GFP), *n*=170	65 (38%)	35 (21%)	22 (13%)	48 (28%)
ice2Δ (Hmg1p-GFP), *n*=251	93 (37%)	48 (19%)	36 (14%)	74 (29%)
Wild type (Sec61p-GFP), *n*=119	0 (0%)	5 (4%)	2 (2%)	112 (94%)
ice2Δ (Sec61p-GFP), *n*=168	28 (17%)	25 (15%)	68 (41%)	47 (28%)

*Small buds: volume of 4-13% of mother cell.

YIL090w encodes a novel protein that is 491 amino acids in length and has a predicted molecular mass of 56.2 kDa. It is also predicted to be a type-III membrane protein that spans the membrane seven times according to the PSORT (Protein Sorting Signals prediction) program and the SOSUI transmembrane segment prediction program, respectively. A BLAST search identified two potential homologues, one with 26% similarity in *S. pombe* (SPAC23C11.0) and another with 34% similarity in *Candida albicans* (IPF12173; orf6.4010). We named the product of YIL090w *ICE2* (inheritance of cortical ER 2) because it was identified in a screen for mutants defective in cortical ER inheritance and maintenance.

Cells lacking Ice2p display defects in the distribution of cortical ER

To confirm that *ICE2* is required for the distribution of ER in mother and daughter cells, the genomic copy of *ICE2* was disrupted in a wild-type strain expressing Hmg1p-GFP (strain SFNY1128, Table 1). The ER distribution defect observed in the *ice2Δ* mutant (strain SFNY1128, Table 1) was similar to the phenotype observed in the *ice2::Tn3* mutant and was

quantified in more than 250 small buds with a volume of 4-13% of the mother cell. Approximately 70% of the cells displayed defects in the distribution of cortical ER (Fig. 1A, right, Table 2). Some of the *ice2Δ* mutant cells lacked ER in small buds (37%; Fig. 1A, right, star), whereas others contained an ER 'dot' (19%; Fig. 1A, right, arrow) or patch (14%; Fig. 1A, right, arrowhead) at the bud tip. Because the phenotype of *ice2Δ* cells is similar to the phenotype of the *ice2::Tn3* mutant, we conclude that the observed defect in cortical ER distribution was due to the absence of the *ICE2* gene and not a consequence of the transposon insertion.

To ensure that the cortical ER distribution defect was not specific to Hmg1p-GFP, a second ER marker was used to examine the distribution of cortical ER in *ice2* mutants. Sec61p is a resident ER integral-membrane protein that is required for the translocation and dislocation of proteins across the ER membrane (Johnson and van Waes, 1999). In wild-type cells, the localization pattern of Sec61p-GFP was similar to Hmg1p-GFP (Fig. 1B, left, Table 2). By contrast, most *ice2Δ* mutant cells contained no ER in buds (Fig. 1B, right, arrow), or accumulated ER (a 'dot' or an ER patch, respectively; Fig. 1B, right, arrow and arrowhead) at the bud tip. Less continuous peripheral ER staining was also observed in the mother cell. Thus, the defect in the distribution of cortical ER in the *ice2Δ* mutant expressing Sec61p-GFP was similar to that of mutant cells expressing Hmg1p-GFP (Table 2), indicating that the observed abnormalities were not specific to Hmg1p-GFP.

Ice2p is an integral membrane protein

ICE2 encodes a putative multiple-span membrane protein. Like other transmembrane proteins that contain multiple membrane-spanning domains, denatured aggregates of Ice2p might form upon boiling in SDS (Blumer et al., 1988; Shimoni et al., 2000). Therefore, to detect Ice2p by western blot analysis, two different solubilization methods were used. Cell lysates were prepared by glass-bead lysis and boiled in SDS-containing sample buffer. Alternatively, lysates were TCA precipitated or prepared in the absence of boiling according to a protocol by Ferreira et al. (Ferreira et al., 2002), which prevents aggregation of the multiple-span yeast membrane protein Pma1p (Mandala and Slayman, 1989). Ice2p was functionally tagged with either GFP or a 13× Myc epitope. Using an affinity-purified polyclonal antibody directed against GFP or a monoclonal antibody directed against the Myc epitope, Ice2p was detected by western blot analysis (Fig. 3A, lanes 1,5). This band was absent from a lysate from an untagged strain, NY873 (Fig. 3A, lanes 2, 4, 6) or when lysates were boiled in SDS-containing sample buffer (Fig. 3A, lane 3). These data suggest that protein aggregates of Ice2p are generated when samples are boiled. Like other integral membrane proteins, Ice2p is solubilized from membranes with Triton X-100 but not with high salt (data not shown).

Predicted topology of Ice2p

Ice2p has two potential glycosylation sites, at amino acids 109-111 and 351-353. To determine whether Ice2p is glycosylated, cell lysates prepared from an untagged strain (NY873, Table 1) and an Ice2p-Myc-

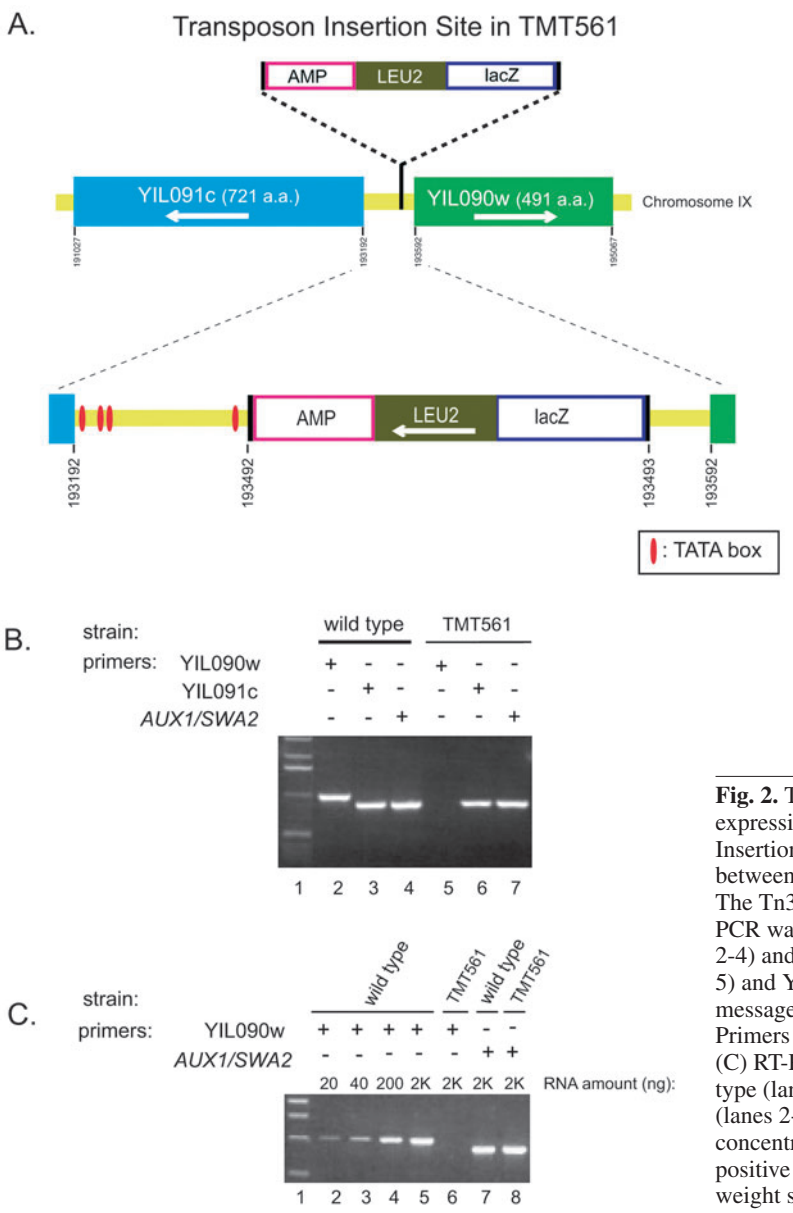

Fig. 2. The transposon insertion specifically affects YIL090w expression. (A) Mapping of the transposon insertion site in TMT561. Insertion of the Tn3 transposon in TMT561 (strain SFNY1052) maps between the ORFs YIL091c and YIL090w on chromosome IX. (B) The Tn3 transposon specifically affects expression of YIL090w. RT-PCR was performed on samples prepared from the wild type (lanes 2-4) and from TMT561 (lanes 5-7). Primers for YIL090w (lanes 2, 5) and YIL091c (lanes 3, 6) were used to determine whether the message levels in either ORF were affected by the Tn3 transposon. Primers for *AUX1/SWA2* were used as a positive control (lanes 4, 7). (C) RT-PCR was performed on RNA samples prepared from wild type (lanes 2-5, 7) and TMT561 (lanes 6, 8). Primers for YIL090w (lanes 2-6) were used to determine message levels at increasing concentrations of RNA. Primers for *AUX1/SWA2* were used as a positive control (lanes 7, 8). Lane 1 in B and C contain the molecular weight standards.

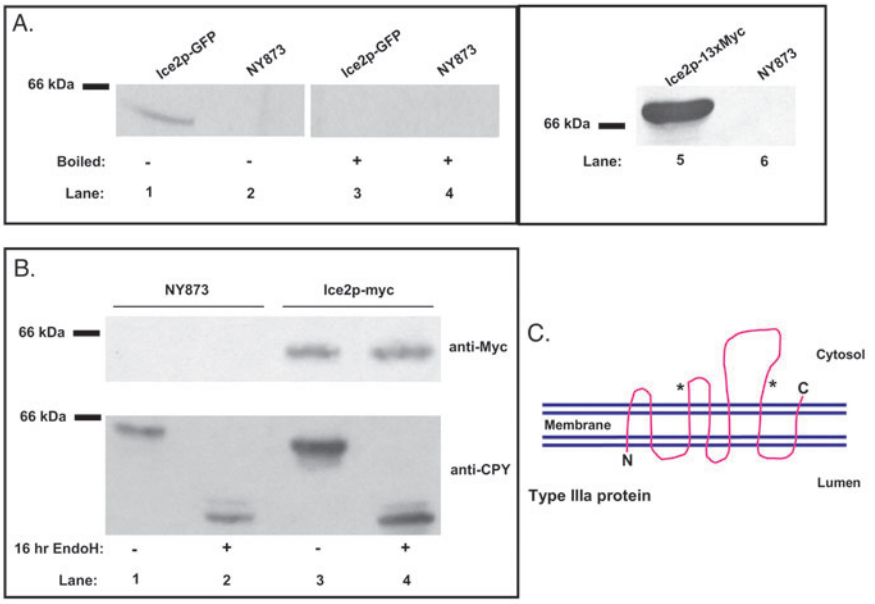

Fig. 3. Predicted topology of Ice2p. (A) Ice2p might aggregate at 100°C. Lysates were prepared from strains SFNY1082 (Ice2p-GFP) and NY873 (an untagged control strain). Protein samples were TCA precipitated and subjected to SDS-PAGE and western blot analysis using an affinity-purified polyclonal antibody directed against GFP (lanes 1,2). A band corresponding to Ice2p-GFP that migrated below the 66 kDa marker was found in lane 1 but not in the untagged control (lane 2). Ice2p-GFP was not detected when samples in lanes 3 and 4 (untagged control) were heated for 5 minutes at 100°C in sample buffer. Lysates were also prepared from a strain in which Ice2p was tagged at its C-terminus with a 13×-Myc epitope. Samples were TCA precipitated, resolved on a 10% SDS-polyacrylamide gel and subjected to immunoblot analysis using monoclonal antibodies directed against the Myc epitope on Ice2p. Lane 5 contains Ice2p-Myc. Lane 6 contains a lysate prepared from an untagged strain (NY873). (B) The mobility of Ice2p was not altered upon EndoH treatment. Lysates from the untagged control and SFNY1283 (Ice2p-Myc) were digested with EndoH (lanes 2, 4) for 16 hours. Samples were resolved by SDS-PAGE and subjected to western blot analysis using anti-Myc (B, top) and anti-CPY antibodies (B, bottom). (C) Schematic of Ice2p topology. Putative glycosylation sites lie in the second and third cytosolic loops of Ice2p (asterisks). This analysis supports the hypothesis that Ice2p is a type-III membrane protein.

tagged strain (SFNY1283, Table 1) were treated with EndoH, which deglycosylates native glycoproteins by removing *N*-linked carbohydrate chains from protein moieties. Digestion with EndoH reduced the molecular mass of CPY, a well-characterized glycoprotein with four *N*-linked glycosylation sites (Ballou et al., 1990) (Fig. 3B, bottom). However the mobility of Ice2p was not altered, suggesting that Ice2p is not glycosylated (Fig. 3B, top).

Proteins are not likely to be glycosylated if potential *N*-linked glycosylation sites are located within transmembrane domains or cytosolic loops, or if the acceptor site is within 12-14 amino acids of the beginning or end of a transmembrane segment (Landolt-Marticorena and Reithmeier, 1994; Nilsson and von Heijne, 1993). If the N-terminus of Ice2p is in the ER lumen and the C-terminus is in the cytosol, the two putative glycosylation sites of Ice2p are predicted to be located on the second and third cytosolic loops (Fig. 3C, asterisks). The finding that Ice2p is not glycosylated provides support for this topology and implies that Ice2p is a type-III integral membrane protein.

Ice2p co-localizes with ER membranes

To begin to determine the localization of Ice2p, subcellular fractionation was performed on sucrose velocity gradients that resolve the ER from other intracellular membranes (Antebi and Fink, 1992; Barrowman et al., 2000). Lysates were prepared from strain SFNY1283 (Table 1) and the fractionation of Ice2p was compared to that of Sec22p, a v-SNARE that is found on both ER and Golgi membranes (Barrowman et al., 2000; Cao and Barlowe, 2000). Ice2p fractionated with the ER peak of Sec22p in fraction 9 (Fig. 4A), implying that Ice2p fractionates with ER, and not Golgi, membranes.

On the sucrose velocity gradients we used, the ER fractionates with the plasma membrane. To resolve these two compartments, the ER was stripped of ribosomes by lysing and fractionating cells on a sucrose density gradient in the presence of EDTA. Stripping the ER of ribosomes alters the density of the ER but not the plasma membrane (Estrada et al., 2003; Roberg et al., 1997). Lysates were prepared from strain SFNY1283 and the distribution of Ice2p was compared by western blot analysis, to that of Sec61p a marker for the ER, and to that of Pma1p, which marks the plasma membrane (Mandala and Slayman, 1989). Ice2p fractionated with the ER, which migrated at the top of this gradient (Fig. 4B, fractions 6-8), and not the plasma membrane (Fig. 4B, fractions 10-13).

In order to confirm the results obtained from subcellular fractionation studies, we used the Ice2p-GFP fusion protein to localize Ice2p in vivo. In Fig. 5A, Ice2p is shown to localize to the region surrounding the nucleus (perinuclear ER) as well as to the cell surface (cortical ER). Indirect immunofluorescence was also performed with cells expressing Ice2p-Myc and the ER marker Hmg1p-GFP. Ice2p-Myc displayed the same staining pattern as Hmg1p-GFP (Fig. 5B, first and second rows). These studies demonstrate that Ice2p localizes with Hmg1p-GFP to the periphery of the cell and the nuclear envelope (Fig. 5B, third row).

Cortical ER network is abnormal in cells lacking Ice2p

Prinz et al. have reported (Prinz et al., 2000) that the cortical ER in yeast forms a dynamic, interconnected tubule network, similar in structure to the ER in higher eukaryotic cells. Because a defect in cortical ER distribution was observed in *ice2* mutant cells, we investigated the ER network at the cell periphery of both mother and daughter cells. Wild-type and *ice2Δ* mutant diploid cells expressing the ER marker Hmg1p-GFP were analysed and images were obtained at the centre of the cell and at the periphery. Wild-type cells exhibited an interconnected, lattice-like tubule network in both the mother

cell and bud (Fig. 6A,D). In approximately 72% of the cells lacking Ice2p, a faint and abnormal ER tubule network was displayed in the developing bud as well as in the mother cell (Fig. 6B,D). To determine whether mutants defective in ER inheritance also displayed an aberrant cortical ER network, the *sec3Δ* diploid mutant was analysed. Although *sec3* mutants lack cortical ER in small buds, 99% of the cells contained a continuous ER network in the mother cell (Fig. 6C,D), reminiscent of the ER network observed in the mother cell of wild type. Previous studies have shown that Sec3p, a

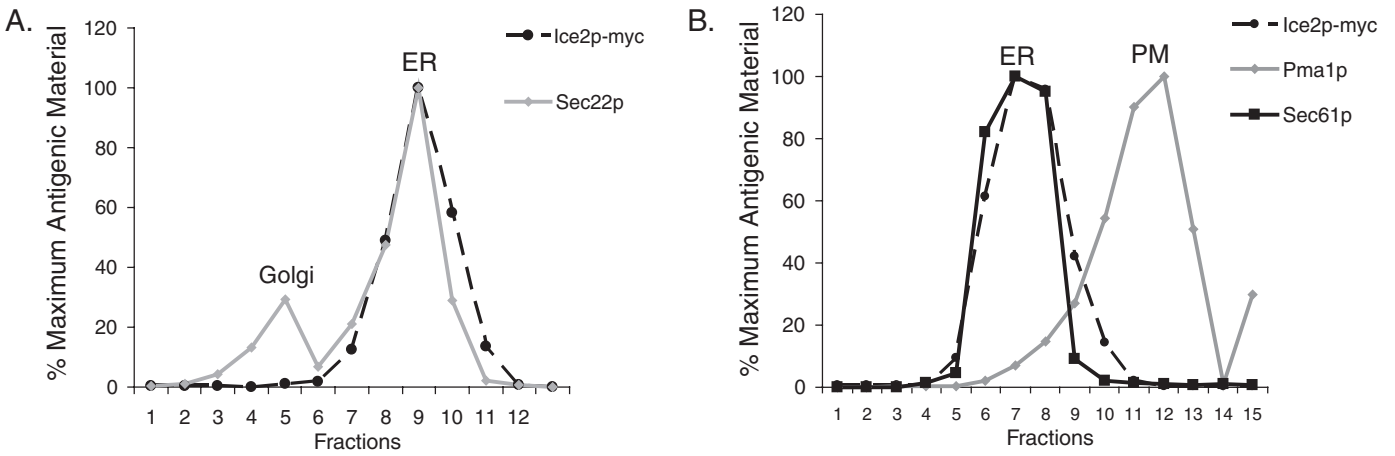

Fig. 4. Ice2p fractionates with the ER and not the plasma membrane. Cells were grown in YPD at 30°C to early log phase. (A) Ice2p-Myc (black dashed line) fractionates with the ER but not the Golgi peak of Sec22p (grey solid line) on a sucrose velocity gradient. (B) Ice2p-Myc (black dashed line) fractionates with the ER marker Sec61p (black solid line), but does not fractionate with the plasma-membrane marker Pma1p (grey solid line) on a sucrose density gradient containing EDTA.

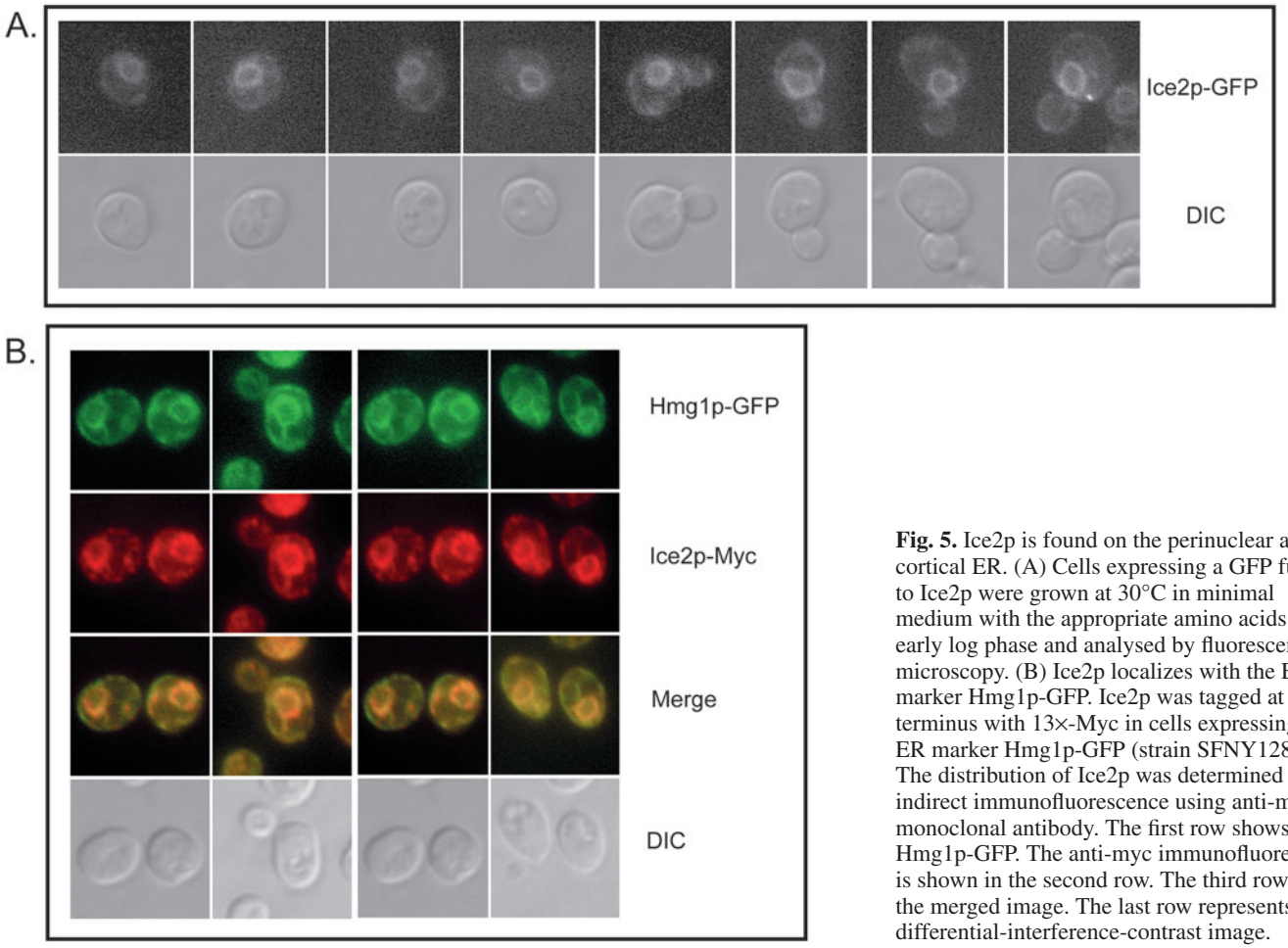

Fig. 5. Ice2p is found on the perinuclear and cortical ER. (A) Cells expressing a GFP fusion to Ice2p were grown at 30°C in minimal medium with the appropriate amino acids to early log phase and analysed by fluorescence microscopy. (B) Ice2p localizes with the ER marker Hmg1p-GFP. Ice2p was tagged at its C-terminus with 13×-Myc in cells expressing the ER marker Hmg1p-GFP (strain SFNY1283). The distribution of Ice2p was determined by indirect immunofluorescence using anti-myc monoclonal antibody. The first row shows Hmg1p-GFP. The anti-myc immunofluorescence is shown in the second row. The third row shows the merged image. The last row represents the differential-interference-contrast image.

component of the multisubunit complex called the exocyst is the putative receptor for cortical ER in daughter cells (Wiederkehr et al., 2003). These findings indicate that disrupting ER inheritance does not affect the cortical ER network. Furthermore, they also suggest that Ice2p might play a role in forming or maintaining the cortical ER network.

To investigate further the nature of the aberrant ER network in *ice2* mutant cells, subcellular fractionation was performed and the ER was identified using the ER markers Sec61p and Hmg1p-GFP. Wild-type ER membranes were found to be most concentrated in fraction 9 in the sucrose velocity gradient described above (Fig. 7A, left and middle). However, the peak of ER membranes obtained from *ice2Δ* cells was shifted to fraction 7 on this gradient (Fig. 7A, left and middle). The

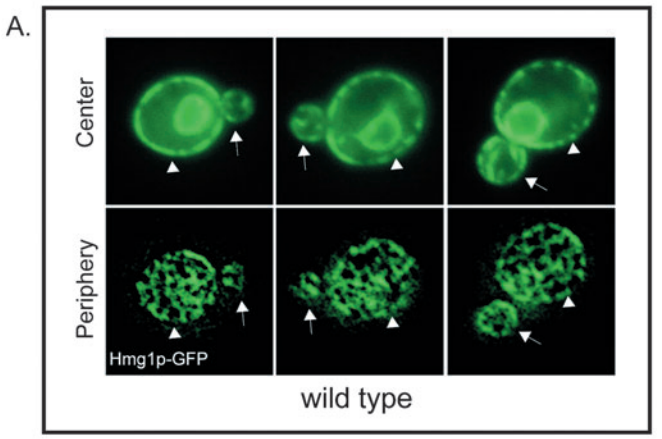

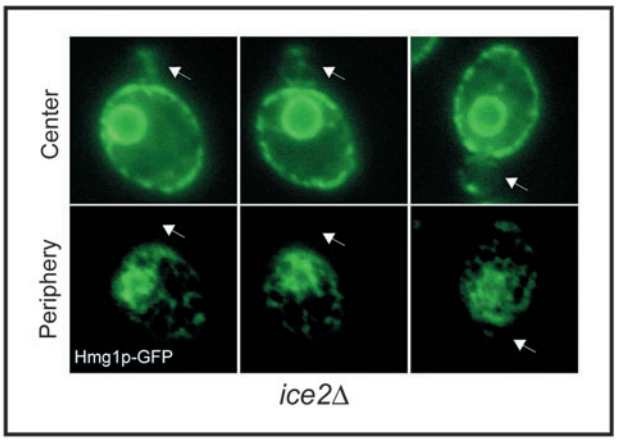

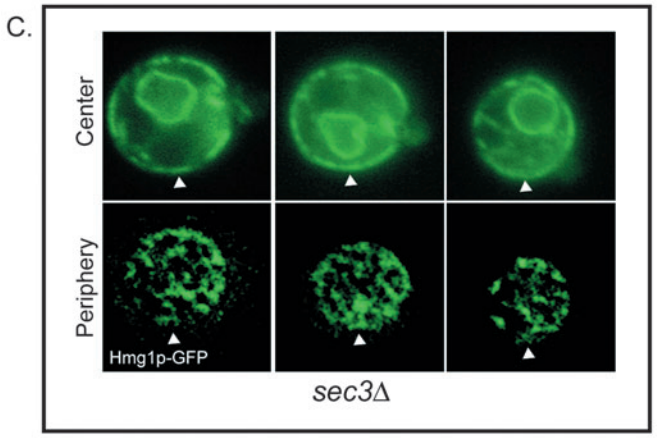

D.

	Normal Network	Abnormal Network
Wild type	83/85 (97.6%)	2/85 (2.4%)
ice2Δ	31/112 (27.7%)	81/112 (72.3%)
sec3Δ	72/73 (98.6%)	1/73 (1.4%)

Fig. 6. The cortical ER tubular network is defective in the *ice2Δ* mutant. Wild-type (strain SFNY1061) (A), *ice2* mutant (strain SFNY1282) (B) and *sec3* mutant (strain SFNY1449) (C) cells expressing the ER marker Hmg1p-GFP were analysed using fluorescence microscopy. Images were obtained from the centre of the cell and from the cell periphery. Arrowheads point to a continuous network displayed in the mother cell (A,C). Arrows point to buds that display a normal cortical ER network (A) and buds that lack an intact cortical ER network (B). An abnormal ER network is observed in the mother cell of the *ice2* mutant (B). (D) Quantitation of wild-type and mutant cells displaying an aberrant cortical ER network.

Fig. 7. ER membranes from *ice2* mutant cells do not fractionate with the ER peak of wild-type membranes. Wild-type (strain SFNY1054) and *ice2Δ* (strain SFNY1128) mutant cells were grown at 30°C in YPD to early log phase and subjected to subcellular fractionation using sucrose velocity (A) and sucrose density gradients (B). Fractions were then subjected to western blot analysis. In the wild type, the ER markers Sec61p (A, left) and Hmg1p-GFP (A, middle), and the ER peak of Bet1p (A, right) were found in fraction 9 (black squares), whereas the ER from *ice2Δ* cells was found in fraction 7 (grey triangles). In wild-type density gradients, the ER markers Sec61p (B, left) and Aux1p (B, middle) were found in fraction 10 (black squares), whereas the ER from *ice2Δ* cells was shifted to the left in fraction 9 (grey triangles). The distribution of the Golgi was not altered in *ice2* mutants (A, right, B, right). (C) ER membranes from the *ice2Δ* mutant fractionate with wild-type ER after cycloheximide treatment. The SFNY1054 and SFNY1128 strains expressing the ER marker Hmg1p-GFP were grown in YPD at 30°C and treated with cycloheximide for 6 hours, and then subcellular fractionation was performed using sucrose density gradients. Western blot analysis demonstrated that the ER markers Sec61p (C, left), Aux1p (C, middle) and Dpm1p (C, right), were in fraction 10 in both wild-type (black triangles) and *ice2Δ* samples (grey squares). (D) Cycloheximide treatment restores the density of *srp102-510* ER membranes to that of the wild type. Wild-type (FY23) and *srp102-510* (WPY152) mutant cells were grown at 25°C in YPD to early log phase, shifted to 37°C for 6 hours in the absence (D, left, middle) or presence (D, right) of cycloheximide (CHX) and subjected to subcellular fractionation using sucrose density gradients. Western blot analysis showed that ER membranes (D, left) from the wild type (black squares) peaked in fraction 10, whereas the ER from *srp102-510* was found in fraction 9 (grey triangles). Upon CHX treatment, the ER marker Dpm1p (D, right) was in fraction 9 in both the wild type (black squares) and *srp102-510* (grey triangles).

distribution of Sec22p, a v-SNARE that is found on both ER and Golgi membranes (Barrowman et al., 2000; Cao and Barlowe, 2000), was examined to determine whether the shift in mutant membranes was specific to the ER. The Golgi peak of Sec22p was localized to fraction 3 in wild-type and *ice2Δ* cells (Fig. 7A, right). However, the ER peak was found in fraction 7 instead of fraction 9 (Fig. 7, right).

Subcellular fractionation using sucrose density gradients was also performed. For wild-type membranes, the ER marker Sec61p (Fig. 7B, left) peaked in fraction 10. The distribution

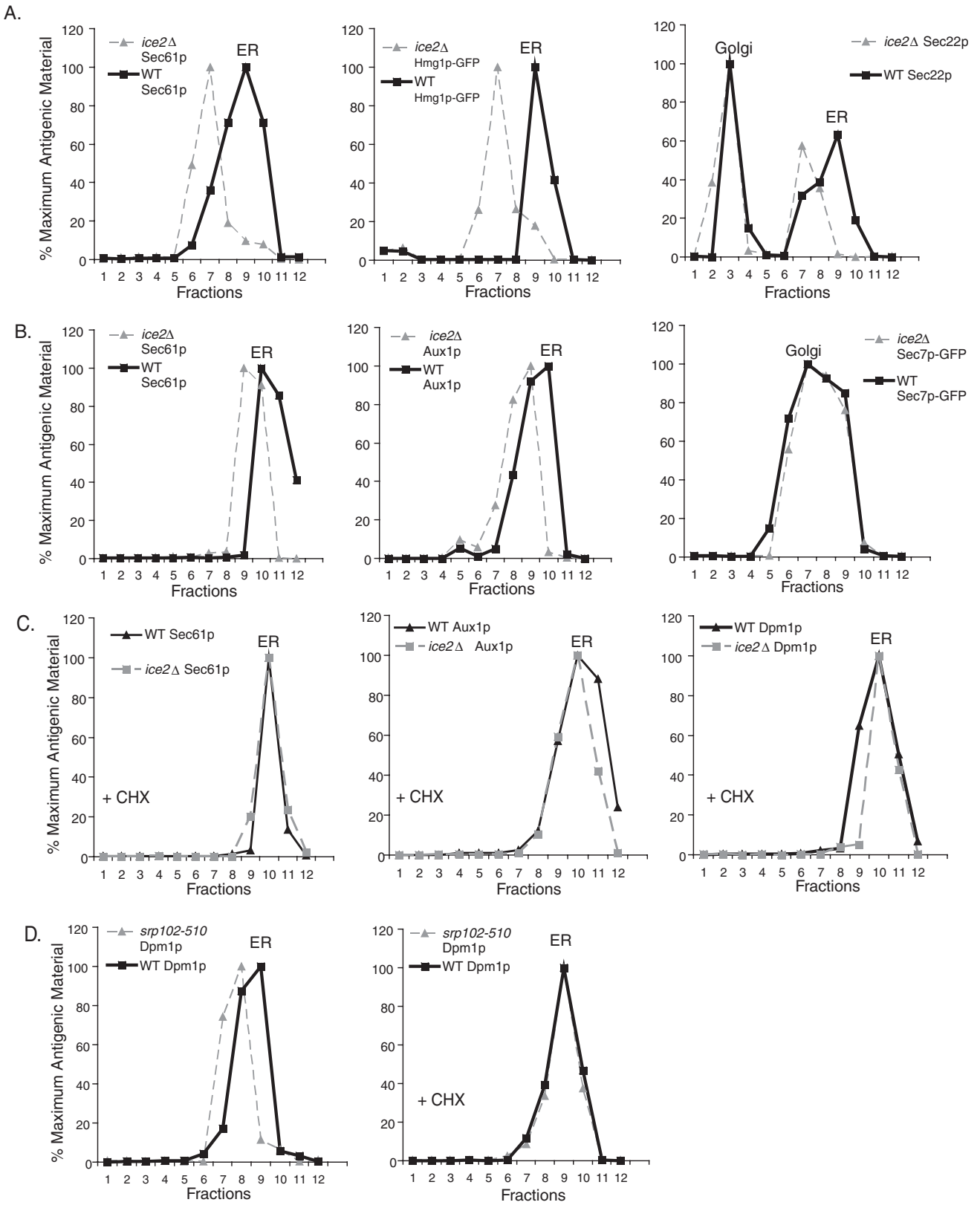

of Aux1p, a hydrophilic ER protein that is required for ER inheritance (Du et al., 2001), was also examined and found to be in fraction 10 (Fig. 7B, middle). By contrast, the ER membranes from *ice2Δ* cells were shifted to fraction 9 on this gradient (Fig. 7B, left and middle). The distribution of the late Golgi marker Sec7p in both wild-type and *ice2Δ* peaked in fraction 7 on sucrose density gradients (Fig. 7B, right). Thus, the loss of Ice2p appears to affect the density of ER, but not Golgi, membranes. These findings support the hypothesis that cells lacking Ice2p have an abnormal ER structure.

Cortical ER network defect in *ice2Δ* is not a consequence of blocking the targeting of ribosomes to the ER

Previous studies have shown that the cortical ER network is abnormal in yeast mutants that are defective in targeting ribosomes to the ER membrane (Prinz et al., 2000). This abnormality can be rescued with cycloheximide, a drug that inhibits protein synthesis. It was postulated that cycloheximide's ability to slow down translation compensates for ribosome binding defects by providing additional time for ribosome/nascent-chain complexes to bind to the ER (Prinz et al., 2000). The abnormal and irregular cortical ER network observed in *ice2* mutants, as well as the altered physical properties of the ER upon sedimentation, might be the consequence of a defect in the association of ribosomes with ER membranes. A severe defect in ribosome binding is unlikely, because *ice2* mutants grow normally and secrete the periplasmic protein invertase efficiently (data not shown). However, to address this possibility further, we determined whether the removal of ribosomes from the ER altered the density of wild-type membranes to the same extent as *ice2Δ* mutant membranes. Lysates were treated with EDTA to remove ribosomes from ER membranes and the fractionation of two ER markers was monitored on sucrose density gradients. In the presence of EDTA, wild-type ER membranes marked by Sec61p (see Fig. S2, left, in supplementary material) and Aux1p (see Fig. S2, right, in supplementary material) sedimented to the same density as the *ice2Δ* mutant membranes. This finding supports the hypothesis that the attachment of ribosomes to ER membranes is at least partially defective in the *ice2Δ* mutant.

The ER distribution might be abnormal in *ice2Δ* cells because of a ribosome-binding defect or ribosome binding to ER membranes might be impaired in the *ice2Δ* mutant because the cortical ER network is defective. To resolve these possibilities, *ice2Δ* cells were treated with cycloheximide and subcellular fractionation, as well as fluorescence microscopy, was performed to analyse the cortical ER network. ER membranes from cycloheximide-treated wild-type and *ice2* mutant cells were resolved on sucrose density gradients. The ER from the *ice2* mutant peaked in fraction 9 before treatment with cycloheximide (Fig. 7B) but migrated with wild-type ER membranes in fraction 10 after treatment (Fig. 7C). This result indicates that the partial ribosome-binding defect in the *ice2* mutant can be rescued with cycloheximide. Prinz et al. reported (Prinz et al., 2000) that mutants of the β subunit of the SRP (signal recognition particle) receptor, *srp102-510*, displayed an abnormal ER network and an altered ER distribution. However, these defects were corrected with cycloheximide. As a control, we also examined the distribution of ER membranes from *srp102-510* cells that were grown in the absence and presence of cycloheximide. ER membranes were found in fraction 9 in wild-type (Fig. 7D). However, as was observed for the *ice2* mutant (Fig. 7B), the peak of ER membranes from *srp102-510* was found in fraction 8 before treatment with cycloheximide (Fig. 7D, left). Treatment with cycloheximide shifted the density of *srp102-510* ER membranes to fraction 9 (Fig. 7D, right). Together, these findings indicate that there is a partial defect in the attachment of ribosomes to ER membranes in the *ice2* mutant.

To determine whether the defect in ribosome binding causes the abnormal ER network in the *ice2* mutant, fluorescence microscopy was performed on mutant cells before and after treatment with cycloheximide. A continuous ER tubule network was observed in the mother cell and bud in 99% of wild-type cells treated with cycloheximide (Fig. 8A, left). By contrast, an irregular and aberrant cortical ER network was observed in the developing bud and mother cell in 72% of *ice2Δ* mutants treated with cycloheximide (Fig. 8A, right). Because this treatment is effective at restoring the ER network and distribution in *srp102-510*, a mutant known to be defective in ribosome binding (Prinz et al., 2000) (see Fig. S3 in supplementary material), we conclude that the abnormal ER network observed in the *ice2Δ* mutant is unlikely to be a consequence of a ribosome-binding defect. Rather, our findings imply that the abnormal structure of the ER might affect the ability of ribosomes to bind to the ER.

Morphology and distribution of mitochondria is unaltered in the *ice2Δ* mutant

An association of the mitochondria with ER membranes has previously been reported (Achleitner et al., 1999; Gaigg et al., 1995; Pitts et al., 1999; Prinz et al., 2000). In mutants that block the translocation of proteins into the ER and traffic between the ER and Golgi (Prinz et al., 2000), the mitochondria were found to be fragmented. To determine whether the morphology of the mitochondria was altered in *ice2Δ* mutants, a mitochondrial targeting sequence fused to RFP (Mozdy et al., 2000) was examined in wild-type and *ice2Δ* cells. In the *ice2Δ* mutant, mitochondria were delivered into 99% of small buds that displayed defects in cortical ER distribution (Fig. 8B, right), whereas 96% of small-budded wild-type cells displayed mitochondrial structures as well (Fig. 8B, left). Mitochondria were also detected at the cell periphery of the mother cell in the mutant as a branched, tubular structure, similar to the mitochondrial structure observed in wild-type cells (Fig. 8B). Thus, the morphology and distribution of mitochondria were indistinguishable in wild-type and *ice2* mutant cells.

Discussion

A genetic screen for mutants defective in the maintenance and/or delivery of cortical ER from the mother cell to the emerging bud has been described previously (Du et al., 2001). This screen resulted in the identification of four genes whose products are involved in these processes. In this study, we characterize the *ICE2* gene product, a novel multispanning integral membrane protein. Fluorescence microscopy has revealed that cells lacking Ice2p failed to maintain or form a

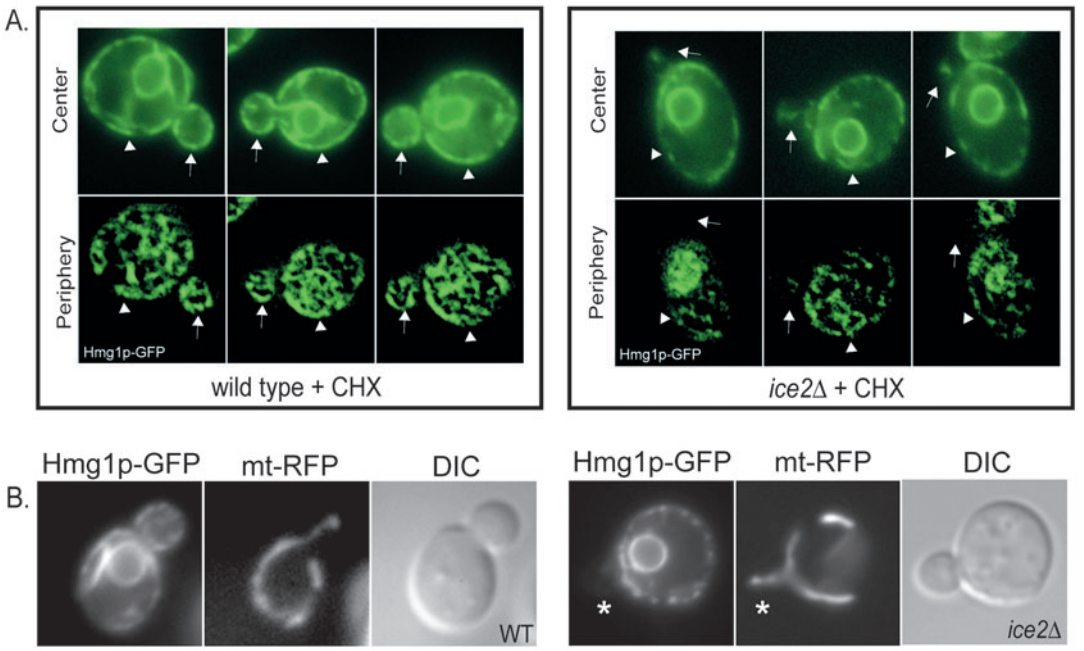

Fig. 8. An aberrant cortical ER network persists after cycloheximide treatment in the *ice2* mutant. (A) The cortical ER network remains abnormal upon cycloheximide treatment in the *ice2Δ* mutant. Diploid cells (strains SFNY1061 and SFNY1282) expressing the ER marker Hmg1p-GFP were grown in YPD at 30°C, treated with cycloheximide for 6 hours and analysed using fluorescence microscopy. Images were obtained from the periphery and centre of the cell. Arrowheads point to a continuous network displayed in wild-type mother cells (A, left). Arrows point to wild-type buds that display a normal cortical ER network (A, left) and to buds in *ice2Δ* cells that lack an intact cortical ER network (A, right). An abnormal ER network (arrowheads) is also observed in the mother cell of the *ice2* mutant (A, right). (B) The mitochondrial structure remains intact in *ice2* mutants displaying an aberrant cortical ER network. Mitochondrial distribution was studied using fluorescence microscopy in wild-type and *ice2Δ* cells expressing the ER marker Hmg1p-GFP (left). Mitochondria were visualized in cells transformed with plasmid SFNB798, which expresses the mitochondrial targeting sequence from the F_0 ATP synthase fused to RFP (middle). The differential-interference-contrast images (DIC) are located on the right. The distribution of mitochondria was determined in small buds with a volume of 4-13% of the mother.

normal ER tubular network, whereas known ER inheritance mutants such as *sec3Δ* (Wiederkehr et al., 2003) and *aux1Δ* (Du et al., 2001) displayed a highly interconnected tubular network (Fig. 6C; data not shown). The *ice2Δ* mutant did not display a growth or secretion defect (data not shown), indicating that protein trafficking between the ER and Golgi complex was unaltered. Biochemical data from sucrose velocity and density gradients support the fluorescence imaging data and imply that Ice2p might play a role in forming or maintaining the structure of the cortical ER network.

ICE2 encodes a transmembrane protein that localizes to the ER. Ice2p-GFP was found at the cell periphery and the perinuclear region, corresponding to the cortical ER and the perinuclear ER, respectively. Huh et al. (Huh et al., 2003) performed a yeast genome-wide GFP-fusion-protein localization study in which 75% of yeast proteins were GFP tagged at their C-termini. The study corroborated our localization results by reporting that Ice2p-GFP localized to both the perinuclear region and cell periphery. Unlike many integral membrane proteins that are found in more than one membrane compartment (Bonifacino and Glick, 2004; Pelham, 1999), Ice2p behaves like a resident ER protein. ER-resident proteins contain a transmembrane domain (TMD) determinant (Letourneur and Cosson, 1998; Sato et al., 1997; Sato et al., 2003) or an HDEL (Munro and Pelham, 1987; Pelham, 1988) or KKXX (Jackson et al., 1990) ER retrieval signal at their C-termini. The length of transmembrane domains has also been implicated in ER retention of C-terminally membrane-anchored ER proteins, such as cytochrome b_5 and the yeast protein Ubc6p (Honsho et al., 1998; Yang et al., 1997). HDEL or KKXX motifs are not found at the C-terminus of Ice2p, but a TMD ER-localization determinant comprised of a hydrophobic amino acid cluster flanked by polar amino acids (Y and S) is located in TMDs I and V. The TMD localization determinant is similar to what has been reported for Sec71p and Sec12p in yeast (Sato et al., 1997; Sato et al., 2003). Thus, Ice2p might be retained in the ER by way of its transmembrane domain.

Work by Prinz et al. (Prinz et al., 2000) has demonstrated that the structural integrity of the cortical ER network is compromised in protein translocation mutants that disrupt the targeting of ribosomes to the ER. This defect can be restored when protein synthesis is inhibited with the drug cycloheximide (Prinz et al., 2000). Although the association of ribosomes with the ER appears to be partially disrupted in *ice2*, an irregular and aberrant cortical ER network is still observed in the presence of cycloheximide. Therefore, the abnormal ER network that is observed in the *ice2* mutant is unlikely to be a consequence of a defect in ribosome binding. In ER-Golgi trafficking mutants and protein translocation mutants that display an abnormal cortical ER network, the mitochondria are also fragmented and disrupted (Prinz et al., 2000). However,

our results show that the morphology and partitioning of the mitochondria is normal in the *ice2* mutant.

Synthetic lethality has been observed upon combination of disruptions in *KAR3* and *ICE2*, suggesting that these gene products work on the same or parallel pathways (Tong et al., 2004). *KAR3* encodes a minus-end-directed microtubule motor protein that localizes to the spindle pole body. Kar3p is essential for nuclear migration and fusion during mating and is believed to cross-link microtubules between fusing nuclei, drawing them together by minus-end-directed forces (Endow et al., 1994; Meluh and Rose, 1990; Middleton and Carbon, 1994). Interestingly, *kar3Δ* cells expressing the ER marker, Hmg1p-GFP, displayed an ER distribution phenotype that was similar to what we observed in the *ice2Δ* mutant (see Fig. S4 in supplementary material). The role that Kar3p might play in forming or maintaining the cortical ER network remains to be determined.

The yeast ER tubular network at the cell periphery is highly dynamic and continuously rearranges. This tubular network is likely to be maintained by ER tubule-tubule fusion (Lin et al., 2001; Prinz et al., 2000). In this study, we have shown that Ice2p is specifically required for the maintenance and distribution of the cortical ER network. Future studies of the maintenance of the cortical ER structure in yeast might provide insight into the mechanism by which Ice2p mediates this process.

We thank Y. Zhang, L. Walker and L. Cavallo for technical assistance, and K. Allen for technical advice. We also thank W. Prinz and T. Rapoport for the *srp102-510* mutant. This work was supported by a program project grant from the National Cancer Institute. Y. Du was an Associate of the Howard Hughes Medical Institute.

References

Achleitner, G., Gaigg, B., Krasser, A., Kainersdorfer, E., Kohlwein, S. D., Perktold, A., Zellnig, G. and Daum, G. (1999). Association between the endoplasmic reticulum and mitochondria of yeast facilitates interorganelle transport of phospholipids through membrane contact. *Eur. J. Biochem.* **264**, 545-553.

Adams, A., Gottschling, D. E., Kaiser, C. A. and Stearns, T. (1997). *Methods in Yeast Genetics*. Cold Spring Harbor, NY: Cold Spring Harbor Laboratory Press.

Antebi, A. and Fink, G. R. (1992). The yeast Ca^{2+}-ATPase homologue, *PMR1*, is required for normal Golgi function and localizes in a novel Golgi-like distribution. *Mol. Biol. Cell* **3**, 633-654.

Ballou, L., Hernandez, L., Alvarado, E. and Ballou, C. (1990). Revision of the oligosaccharide structures of yeast carboxypeptidase Y. *Proc. Natl. Acad. Sci. USA* **87**, 3368-3372.

Barrowman, J., Sacher, M. and Ferro-Novick, S. (2000). TRAPP stably associates with the Golgi and is required for vesicle docking. *EMBO J.* **19**, 862-869.

Blumer, K., Reneke, J. and Thorner, J. (1988). The *STE2* gene product is the ligand-binding component of the alpha-factor receptor of Saccharomyces cerevisiae. *J. Biol. Chem.* **263**, 10836-10842.

Bonifacino, J. S. and Glick, B. S. (2004). The mechanisms of vesicle budding and fusion. *Cell* **116**, 153-166.

Burns, N., Grimwade, B., Ross-Macdonald, P. B., Choi, E. Y., Finberg, K., Roeder, G. S. and Snyder, M. (1994). Large-scale analysis of gene expression, protein localization, and gene disruption in Saccharomyces cerevisiae. *Genes Dev.* **8**, 1087-1105.

Cao, X. and Barlowe, C. (2000). Asymmetric requirements for a Rab GTPase and SNARE proteins in fusion of COPII vesicles with acceptor membranes. *J. Cell Biol.* **149**, 55-66.

Cronin, S. R., Khoury, A., Ferry, D. K. and Hampton, R. Y. (2000). Regulation of HMG-CoA reductase degradation requires the P-type ATPase Cod1p/Spf1p. *J. Cell Biol.* **148**, 915-924.

Du, Y., Pypaert, M., Novick, P. and Ferro-Novick, S. (2001). Aux1p/Swa2p is required for cortical endoplasmic reticulum inheritance in *Saccharomyces cerevisiae*. *Mol. Biol. Cell* **12**, 2614-2628.

Endow, S. A., Kang, S. J., Satterwhite, L. L., Rose, M. D., Skeen, V. P. and Salmon, E. D. (1994). Yeast Kar3 is a minus-end microtubule motor protein that destabilizes microtubules preferentially at the minus ends. *EMBO J.* **13**, 2708-2713.

Estrada, P., Kim, J., Coleman, J., Walker, L., Dunn, B., Takizawa, P., Novick, P. and Ferro-Novick, S. (2003). Myo4p and She3p are required for cortical ER inheritance in *Saccharomyces cerevisiae*. *J. Cell Biol.* **163**, 1255-1266.

Ferreira, T., Mason, A. B., Pypaert, M., Allen, K. E. and Slayman, C. W. (2002). Quality control in the yeast secretory pathway. A misfolded PMA1 H+-ATPase reveals two checkpoints. *J. Biol. Chem.* **277**, 21027-21040.

Friedmann, E., Salzberg, Y., Weinberger, A., Shaltiel, S. and Gerst, J. E. (2002). *YOS9*, the putative yeast homolog of a gene amplified in osteosarcomas, is involved in the endoplasmic reticulum (ER)-Golgi transport of GPI-anchored proteins. *J. Biol. Chem.* **277**, 35274-35281.

Gaigg, B., Simbeni, R., Hrastnik, C., Paltauf, F. and Daum, G. (1995). Characterization of a microsomal subfraction associated with mitochondria of the yeast, *Saccharomyces cerevisiae*. Involvement in synthesis and import of phospholipids into mitochondria. *Biochim. Biophys. Acta* **1234**, 214-220.

Hampton, R. Y., Koning, A., Wright, R. and Rine, J. (1996). In vivo examination of membrane protein localization and degradation with green fluorescent protein. *Proc. Natl. Acad. Sci. USA* **93**, 828-833.

Honsho, M., Mitoma, J.-Y. and Ito, A. (1998). Retention of cytochrome b_5 in the endoplasmic reticulum is transmembrane and luminal domain-dependent. *J. Biol. Chem.* **273**, 20860-20866.

Huh, W. K., Falvo, J. V., Gerke, L. C., Carroll, A. S., Howson, R. W., Weissman, J. S. and O'Shea, E. K. (2003). Global analysis of protein localization in budding yeast. *Nature* **425**, 686-691.

Jackson, M. R., Nilsson, T. and Peterson, P. A. (1990). Identification of a consensus motif for retention of transmembrane proteins in the endoplasmic reticulum. *EMBO J.* **9**, 3153-3162.

Johnson, A. E. and van Waes, M. A. (1999). The translocon: a dynamic gateway at the ER membrane. *Annu. Rev. Cell Dev. Biol.* **15**, 799-842.

Landolt-Marticorena, C. and Reithmeier, R. (1994). Asparagine-linked oligosaccharides are localized to single extracytosolic segments in multi-span membrane glycoproteins. *Biochem. J.* **302**, 253-260.

Lee, C. and Chen, L. B. (1988). Dynamic behavior of endoplasmic reticulum in living cells. *Cell* **54**, 37-46.

Letourneur, F. and Cosson, P. (1998). Targeting to the endoplasmic reticulum in yeast cells by determinants present in transmembrane domains. *J. Biol. Chem.* **273**, 33273-33278.

Lin, A., Patel, S. and Latterich, M. (2001). Regulation of organelle membrane fusion by Pkc1p. *Traffic* **2**, 698-704.

Longtine, M. S., Mckenzie, A., III, Demarini, D. J., Shah, N. G., Wach, A., Brachat, A., Philippsen, P. and Pringle, J. R. (1998). Additional modules for versatile and economical PCR-based gene deletion and modification in *Saccharomyces cerevisiae*. *Yeast* **14**, 953-961.

Mandala, S. and Slayman, C. (1989). The amino and carboxyl termini of the *Neurospora* plasma membrane H^+-ATPase are cytoplasmically located. *J. Biol. Chem.* **264**, 16276-16281.

Meluh, P. and Rose, M. (1990). *KAR3*, a kinesin-related gene required for yeast nuclear fusion. *Cell* **60**, 1029-1041.

Middleton, K. and Carbon, J. (1994). *KAR3*-encoded kinesin is a minus-end-directed motor that functions with centromere binding proteins (CBF3) on an in vitro yeast kinetochore. *Proc. Natl. Acad. Sci. USA* **91**, 7212-7216.

Mozdy, A. D., McCaffery, J. M. and Shaw, J. M. (2000). Dnm1p GTPase-mediated mitochondrial fission is a multi-step process requiring the novel integral membrane component Fis1p. *J. Cell Biol.* **151**, 367-380.

Munro, S. and Pelham, H. R. (1987). A C-terminal signal prevents secretion of luminal ER proteins. *Cell* **48**, 899-907.

Nilsson, I. and von Heijne, G. (1993). Determination of the distance between the oligosaccharyltransferase active site and the endoplasmic reticulum membrane. *J. Biol. Chem.* **268**, 5798-5801.

Palade, G. (1956). The endoplasmic reticulum. *J. Biophys. Biochem. Cytol.* **2**, 85-97.

Pelham, H. R. (1988). Evidence that luminal ER proteins are sorted from secreted proteins in a post-ER compartment. *EMBO J.* **7**, 913-918.

Pelham, H. R. (1999). SNAREs and the secretory pathway – lessons from yeast. *Exp. Cell Res.* **247**, 1-8.

Pitts, K. R., Yoon, Y., Krueger, E. W. and McNiven, M. A. (1999). The dynamin-like protein DLP1 is essential for normal distribution and

morphology of the endoplasmic reticulum and mitochondria in mammalian cells. *Mol. Biol. Cell* **10**, 4403-4417.

Preuss, D., Mulholland, J., Kaiser, C. A., Orlean, P., Albright, C., Rose, M. D., Robbins, P. W. and Botstein, D. (1991). Structure of the yeast endoplasmic reticulum: localization of ER proteins using immunofluorescence and immunoelectron microscopy. *Yeast* **7**, 891-911.

Prinz, W. A., Grzyb, L., Veenhuis, M., Kahana, J. A., Silver, P. A. and Rapoport, T. A. (2000). Mutants affecting the structure of the cortical endoplasmic reticulum in Saccharomyces cerevisiae. *J. Cell Biol.* **150**, 461-474.

Roberg, K. J., Rowley, N. and Kaiser, C. A. (1997). Physiological regulation of membrane protein sorting late in the secretory pathway of *Saccharomyces cerevisiae*. *J. Cell Biol.* **137**, 1469-1482.

Roberg, K. J., Crotwell, M., Espenshade, P., Gimeno, R. and Kaiser, C. A. (1999). *LST1* is a *SEC24* homologue used for selective export of the plasma membrane ATPase from the endoplasmic reticulum. *J. Cell Biol.* **145**, 659-672.

Rose, M. D., Misra, L. M. and Vogel, J. P. (1989). *KAR2*, a karyogamy gene, is the yeast homolog of the mammalian *BiP/GRP78* gene. *Cell* **57**, 1211-1221.

Sato, K., Sato, M. and Nakano, A. (1997). Rer1p as common machinery for the endoplasmic reticulum localization of membrane proteins. *Proc. Natl. Acad. Sci. USA* **94**, 9693-9698.

Sato, K., Sato, M. and Nakano, A. (2003). Rer1p, a retrieval receptor for ER membrane proteins, recognizes transmembrane domains in multiple modes. *Mol. Biol. Cell* **14**, 3605-3616.

Shimoni, Y., Kurihara, T., Ravazzola, M., Amherdt, M., Orci, L. and Schekman, R. (2000). Lst1p and Sec24p cooperate in sorting of the plasma membrane ATPase into COPII vesicles in Saccharomyces cerevisiae. *J. Cell Biol.* **151**, 973-984.

Terasaki, M. (1990). Recent progress on structural interactions of the endoplasmic reticulum. *Cell Motil. Cytoskeleton* **15**, 71-75.

Terasaki, M., Chen, L. and Fujiwara, K. (1986). Microtubules and the endoplasmic reticulum are highly interdependent structures. *J. Cell Biol.* **103**, 1557-1568.

Tong, A. H. Y., Lesage, G., Bader, G. D., Ding, H., Xu, H., Xin, X., Young, J., Berriz, G. F., Brost, R. L., Chang, M. et al. (2004). Global mapping of the yeast genetic interaction network. *Science* **303**, 808-813.

Wiederkehr, A., Du, Y., Pypaert, M., Ferro-Novick, S. and Novick, P. (2003). Sec3p is needed for the spatial regulation of secretion and for the inheritance of the cortical endoplasmic reticulum. *Mol. Biol. Cell* **14**, 4770-4782.

Yang, M., Ellenberg, J., Bonifacino, J. S. and Weissman, A. M. (1997). The transmembrane domain of a carboxyl-terminal anchored protein determines localization to the endoplasmic reticulum. *J. Biol. Chem.* **272**, 1970-1975.